Radiation-Pattern Improvement of Patch Antennas on a Large-Size Substrate Using a Compact Soft Surface Structure and its Realization on LTCC Multilayer Technology

RongLin Li, *Senior Member, IEEE*, Gerald DeJean, *Student Member, IEEE*, Manos M. Tentzeris, *Senior Member, IEEE*, John Papapolymerou, *Senior Member, IEEE*, and Joy Laskar, *Senior Member, IEEE*

Georgia Electronic Design Center
School of Electrical and Computer Engineering
Georgia Institute of Technology
Atlanta, GA 30332-250, U.S.A.
E-mail: rlli@ece.gatech.edu
Phone: 404-385-6003
Fax: 404-894-0222

Abstract— The radiation performance of patch antennas on a large-size substrate can be significantly degraded by the diffraction of surface waves at the edge of the substrate. Most of modern techniques for the surface-wave suppression are related to periodic structures, such as photonic band-gap (PBG) or electromagnetic band-gap (EBG) geometries, which require complicated processes and considerable area. The concept of artificially soft surfaces has been proposed to suppress the surface-wave propagation since the 1990s. However, the typical corrugated soft surface only applies to a substrate whose thickness is one quarter guided wavelength. In this paper, a compact soft surface structure consisting of a square ring of short-circuited metal strips is employed to surround the patch antenna for blocking the surface-wave propagation, thus alleviating the effect of the edge diffraction and hence improving the radiation pattern. Since its operating frequency is determined by the width of the metal strip (about a quarter guided wavelength), the compact soft surface structure is suitable for a substrate with arbitrary thickness and dielectric constant. More importantly, the compact soft surface can be realized on any via-metallization

incorporated packaging process, such as liquid crystal polymer (LCP), multilayer organic (MLO), or low temperature co-fired ceramic (LTCC) technology. A numerical investigation for a patch antenna surrounded by an ideal compact soft surface is presented and the feasibility of its implementation on LTCC technology is demonstrated. It is shown that the gain at broadside of a patch antenna on a thick and large-size substrate can be increased to near 9 dBi through the use of the proposed compact soft surface structure.

Index terms— *Soft surface, surface-wave suppression, radiation-pattern improvement, patch antenna, LTCC technology.*

I. Introduction

In modern wireless sensor and communication systems, there is an increasing demand for integration of antennas not only with radio-frequency (RF) front-end circuits but also with intermediate-frequency (IF) or even base-band (including analog and digital signals) components [1]. Due to its low cost, lightweight, and planar structure, a patch antenna probably is the most likely candidate for this integration. Especially for high-frequency (such as millimeter-wave) applications, the size of a patch antenna may be much smaller compared to the printed circuit board (PCB) substrate, where the analog and digital devices are integrated. When a patch antenna is fabricated on a larger-size substrate, its radiation pattern may be considerably affected (such as dips near the maximum and significant sidelobes) by the diffraction of surface waves at the edge of the finite grounded substrate [2]-[4], particularly when the patch is printed on material with a high dielectric constant, such as gallium arsenide [5] or silicon [6]. On the

other hand, the excitation of strong surface waves also causes unwanted coupling between the antenna and other components on the PCB, thus degrading the performance of the integrated module [7]. This problem is further accentuated in three-dimensional (3D) multilayer compact modules [8].

The most popular technique for the improvement of the radiation performance of patch antennas on a large-size substrate is to construct an artificial periodic structure, such as photonic bandgap (PBG) or electromagnetic bandgap (EBG) [9]-[16], surrounding the patch antenna to prevent the surface waves from propagating in the substrate. Unfortunately, it requires a considerable area to form a complete band gap structure. Typically, to form a band gap at least three periods are required with a period being on the order of a wavelength [17]. In addition, it is usually difficult for most printed-circuit technologies to realize such a perforated structure. Another considered approach has been to lower the effective dielectric constant of the substrate under the patch to prevent energy from being trapped in the substrate, thus allowing for more effective radiation [18], [19]. This approach requires complicated micromachining techniques (such as wet or try etching) and results in a fragile module since the patch is suspended over an air trench.

It has been demonstrated that the concept of artificially soft surfaces can be introduced to improve the radiation patterns for different types of antennas [20], [21]. This technique can be implemented on standard board materials or using emerging multilayer technologies, such as liquid crystal polymer (LCP), multilayer organic (MLO), and low temperature co-fired ceramic (LTCC) processes. However, the conventional soft surface concept based on corrugated structures requires a substrate thickness of one quarter guided wavelength as well as a quite large area [22].

Recently, a modern realization of artificially soft surface structures has been proposed in [23]. The new proposed soft surface consists of a number of quarter-wavelength metal strips that are short-circuited to the ground plane. The operating frequency for this soft surface is determined by the strip width, not by the thickness of the substrate, thus allowing for its implementation in a substrate with arbitrary thickness.

In this paper, we apply the concept of the modern soft surface to improve the radiation pattern of patch antennas. A single square ring of the shorted quarter-wavelength metal strips is employed to form a soft surface and to surround the patch antenna for the suppression of outward propagating surface waves, thus alleviating the diffraction at the edge of the substrate. Since only a single ring of metal strips is involved, the formed soft surface structure is compact and easily integrable with 3D modules. A numerical investigation is presented for a patch antenna surrounded by an ideal compact soft surface structure for three different dielectric substrates. The effectiveness of the compact soft surface in terms of radiation pattern improvement is verified by its implementation on LTCC multilayer technology.

II. Investigation of a Patch Antenna Surrounded by an Ideal Compact Soft Surface Structure

For the sake of simplicity, we consider a probe-fed square patch antenna on a square grounded substrate with thickness *H* and a dielectric constant ε_r. The patch antenna is surrounded by a square ring of metal strip which is short-circuited to the ground plane by a metal wall along the outer edge of the ring, as shown in Fig. 1. The shorted square ring represents an ideal soft surface structure when the width of the metal strip (W_s) is approximately equal to a quarter of the guided wavelength [23]:

$$W_s \cong \frac{\lambda_g}{4} = \frac{c}{4 f_0 \sqrt{\varepsilon_r}} \tag{1}$$

where f_0 is the operating frequency, λ_g is the guided wavelength, and c=3×10^8 m/s. Taking into account the effect of fringing field at the inner edge of the shorted ring, we obtain the following design value for W_s [24]:

$$W_s = \frac{c}{4 f_0 \sqrt{\varepsilon_{re}}} - \Delta W_s \tag{2}$$

where ε_{re} is the effective dielectric constant given by

$$\varepsilon_{re} = \left[\frac{\varepsilon_r + 1}{2} + \frac{\varepsilon_r - 1}{2} F(W_s / H) \right] \tag{3}$$

with

$$F(W_s / h) = (1 + 6H / W_s)^{-1/2}. \tag{4}$$

ΔW_s is an empirical correction factor obtained as

$$\Delta W_s = H \cdot \left[0.882 + \frac{0.164(\varepsilon_r - 1)}{\varepsilon_r^2} + \frac{\varepsilon_r + 1}{\pi \varepsilon_r} \left\{ 0.758 + \ln\left(\frac{2W_s}{H} + 1.88 \right) \right\} \right]. \tag{5}$$

The design value for W_s is optimized by simulation for a maximum directivity at broadside (the z direction).

To demonstrate the effectiveness of the compact soft surface structure on the radiation pattern improvement, we simulated the soft-surface-surrounded patch antenna for three different dielectric constants: ε_r=2.9, 5.4, and 9.6, which correspond to the typical values of LCP and two types of LTCC materials, respectively. The operating frequency is assumed to be f_0=15 GHz. The substrate thickness H is assumed to be 0.5 mm (0.025λ_0, λ_0= the free-space wavelength) and the lateral size (L × L) of the substrate is 40 mm × 40 mm (2λ_0 × 2λ_0), much larger than the size (<0.5λ_g

× $0.5\lambda_g$) of the square patch. The numerical simulation tool used is the TLM (transmission line matrix) based software: *Microstripes 6.0*. For comparison, we also simulated the patch antenna without the soft surface. The patch lengths were found to be L_p=5.4, 3.94, and 2.9 mm respectively for ε_r=2.9, 5.4, and 9.6 at f_0=15 GHz. The optimized (for a maximum directivity) values of W_s are 2.65, 1.88, and 1.36 mm respectively for ε_r=2.9, 5.4, and 9.6, close to the analytically calculated design values: 2.75, 1.93, and 1.35 mm. An important observation following the simulation is that the maximum directivity is quite dependent on the inner length, L_s, of the soft surface ring. Fig. 2 shows the directivity as a function of L_s. We can see the maximum directivity values of 9.6, 9.2, and 9.1 dBi obtained at L_s=24, 22, and 20 mm for ε_r=2.9, 5.4, and 9.6, respectively. The reason for the dependence will be explained later in this section. Note that the maximum directivity was found in [10] to be 8.8 dBi for a patch antenna (on a substrate with ε_r=10) surrounded by a PBG ring with a ring width of ~ $2.5\lambda_g$, ten times of the width of the soft surface ring (~$0.25\lambda_g$).

Since both the patch antenna and the soft surface ring are resonant structures, the directivity is definitely related to the frequency. The relationship is plotted in Fig. 3 for an optimized soft surface structure. The variation of directivity with frequency is slightly smaller for ε_r=2.9 than those for ε_r=5.4 and 9.6. A comparison of return loss between the patch antennas with and without the soft surface is shown in Fig. 4 for ε_r=2.9. It is observed that the soft surface structure has no significant effect on the impedance performance of the patch antenna since the soft surface ring is almost half a wavelength away from the edge of the patch. This observation also applies to the cases for ε_r=5.4 and 9.6.

Next, we proceed to the evaluation of the radiation-pattern improvement achieved by the soft surface structure. The radiation patterns for ε_r=9.6 plotted in two principal planes (E-plane and H-plane) are compared in Fig. 5 between the patch antennas with and without the soft surface. It is seen that without the soft surface the direction for the maximum radiation is no longer in the z-direction due to the contribution from the surface-wave diffraction. By introducing the soft surface structure, the radiation pattern is significantly improved, including enhanced radiation field in the z-direction, narrowed beamwidth in the E plane, and reduced backside radiation. The directivity at broadside is increased by more than 5 dB (from 4.0 dBi to 9.1 dBi) while the backside radiation level gets reduced by about 8 dB. A similar radiation-pattern improvement by the soft surface is observed for ε_r=2.9 and 5.4, where the directivity at broadside increases from 5.7 dBi and 4.5 dBi to 9.6 dBi and 9.2 dBi, respectively.

The mechanism for the radiation pattern improvement achieved by the introduction of a compact soft surface structure can be understood by considering two factors. First the quarter-wave shorted metal strip serves as an open circuit for the TM_{10} mode (the fundamental operating mode for a patch antenna). Therefore, it is difficult for the surface current on the inner edge of the soft surface ring to flow outward (also see Fig. 1). As a result, the surface waves can be considerably suppressed outside the soft surface ring, hence reducing the undesirable diffraction at the edge of the grounded substrate. This explanation can be confirmed by checking the field distribution in the substrate. Fig. 6 shows the electric field distributions on the top surface of the substrate for the patch antennas with and without the soft surface. We can see that the electric field is indeed contained inside the soft surface ring. It is estimated that the

field magnitude outside the ring is approximately 5 dB lower than that without the soft surface.

The second factor contributing to the radiation pattern improvement is the fringing field along the inner edge of the soft surface ring. This fringing field along with the fringing field at the radiating edges of the patch antenna forms an antenna array in the E-plane. The formed array acts as a broadside array with minimum radiation in the x-y plane when the distance between the inner edge of the soft surface ring and its nearby radiating edge of the patch is roughly half a wavelength in free space. Even though the magnitude of the fringing field along the soft surface may be much lower compared to that at the radiating edges, the size of the soft surface ring is much larger than the patch. As a result, the contribution from the soft surface ring to the radiated field at broadside may be significant. Therefore the radiation pattern can be considerably improved by the soft surface ring. Note that if the inner length of the soft surface ring (L_s) is further increased the fringing field will become weaker. Therefore there is an optimized value for L_s. By simulation, it is found that the optimized L_s is approximately equal to one wavelength in free space plus the length of the patch antenna (L_p). In this sense, the soft surface ring is also designed as a radiating element that launches the impinging surface wave into free space and in doing so effectively increases the size of the radiation aperture. By simulation, it is observed that the radiation pattern cannot be further improved by adding more soft surface rings, which supports the claim that the soft surface ring indeed acts as a radiating element.

III. Implementation of the Compact Soft Surface Structure on LTCC multilayer Technology

The LTCC laminated technology is getting more and more popular in wireless and mm-wave applications due to its easy realization of highly integrated, complex multilayer 3D modules and circuits. This technology is appreciated for its flexibility in connecting an arbitrary number of layers with via holes (or via metallization). By using the LTCC technology it is easy to realize the shorting wall required by the compact soft surface structure, minimizing the parasitic surface currents. To demonstrate the feasibility of this technology on the implementation of the soft surface, we first simulated a benchmarking prototype that was constructed to replace the shorting wall with a ring of vias. Note that the LTCC substrate is hidden in order to see the via-related structures clearly. The utilized LTCC material had a dielectric constant of 5.4. The whole module consists of a total of 11 LTCC layers (layer thickness=100 μm) and 12 metal layers (layer thickness=10 μm). The diameter of each via was specified by the fabrication process to be 100 μm and the distance between the centers of two adjacent vias was 500 μm. To support the vias, a metal pad is required on each metal layer. To simplify the simulation, all pads on each metal layer are connected by a metal strip with a width of 600 μm. Simulation showed that the width pad metal strips has little effect on the performance of the soft surface structure as long as it is less than the width of metal strips for the soft surface ring (W_s).

The size of the LTCC board was 30 mm × 30 mm. The operating frequency was set within the K_u band (the design frequency f_0=16.5 GHz). The design value of the distance (i.e. W_s) between the center of the vias and the inner edge of the soft surface ring was estimated by (2). The optimized values for L_s and W_s were respectively 22.2 mm and 1.4 mm, which led to a total via number of 200 (51 vias on each side of the

square ring). Including the width (300 μm) of the pad metal strip, the total metal strip width for the soft surface ring was found to be 1.7 mm.

Since the substrate was electrically thick at f_0=16.5 GHz (>0.1λ_g), a stacked configuration was adopted for the patch antenna to improve its input impedance performance. By adjusting the distance between the stacked square patches, a broadband characteristic for the return loss can be achieved [25]. For the present case, the upper and lower patches (with the same size 3.4 mm × 3.4 mm) were respectively printed on the first LTCC layer and the seventh layer from the top, leaving a distance between the two patches of 6 LTCC layers. The lower patch was connected by a via hole to a 50-Ω microstrip feed line that is on the bottom surface of the LTCC substrate. The ground plane was embedded between the second and third LTCC layers from the bottom. This means that among the total 11 LTCC layers, two were used for the microstrip feed line whereas nine layers for the patch antenna and the soft surface structure. Fig. 7 shows the layout and a prototype of the stacked-patch antenna surrounded by a compact soft surface structure implemented on the LTCC technology. The inner conductor of an SMA (semi-miniaturized type-A) connector was connected to the microstrip feed line while its outer conductor was soldered on the bottom of the LTCC board to a pair of pads that were shorted to the ground through via metallization. Note that the microstrip feed line was printed on the bottom of the LTCC substrate to avoid its interference with the soft surface ring and to alleviate the contribution of its spurious radiation to the radiation pattern at broadside. For comparison the same stacked patch antenna on the LTCC substrate but without the soft surface ring was also built.

The simulated and measured results for the return loss are shown in Fig. 8 and good agreement is observed. Note that because the impedance performance of the stacked-patch antenna is dominated by the coupling between the lower and upper patches, the return loss for the stacked-patch antenna seems more sensitive to the soft surface structure than that for the previous thinner single patch antenna. Fortunately the bandwidth is indeed improved both for the stacked patches with and without the soft surface. The measured return loss is close to -10 dB over the frequency range 15.8-17.4 GHz (about 9% in bandwidth). The slight discrepancy between the measured and simulated results is mainly due to the fabrication issues (such as the variation of dielectric constant or/and the deviation of via positions) and the effect of the transition between the microstrip line and the SMA connector. It is also noted that there is a frequency shift of about 0.3 GHz (about 1.5% up). This may probably be caused by the LTCC material which may have a real dielectric constant a little bit lower than the over estimated design value. Note that it is normal for practical dielectric substrates to have a dielectric constant with ±2% deviation.

The radiation patterns measured in the E- and H-planes are compared with simulated results in Fig. 9. The radiation patterns compared here are for a frequency of 17 GHz where the maximum gain of the patch antenna with the soft surface was observed. From Fig. 9, we can see good agreement for the co-polarized components. It is confirmed that the radiation at broadside is enhanced and the backside level is reduced. Also the beamwidth in the E-plane is significantly reduced by the soft surface. It is noted that the measured cross-polarized component has a higher level and more ripples than the simulation result. This is because the simulated radiation patterns were plotted in two ideal principal planes, i.e. ϕ=0° and ϕ=90° planes. From

simulation, we found that the maximum cross-polarization may happen in the plane ϕ=45° or ϕ=135°. During measurement, a slight deviation from the ideal planes can cause a considerable variation for the cross-polarized component since the spatial variation of the cross-polarization is quick and irregular. Also, a slight polarization mismatch or/and some objects nearby the antenna (such as the connector or/and the connection cable) may considerably contribute to the high cross-polarization.

Finally let us compare the gains between the stacked-patch antennas with and without the soft surface. The simulated and measured gains at broadside (i.e. the z-direction) are shown in Fig. 10. The simulated gain was obtained from the numerically calculated directivity in the z-direction and the simulated radiation efficiency, which is defined as the radiated power divided by the radiation power plus the ohmic loss from the substrate and metal structures ($\tan\delta$=0.002 and $\sigma=5.8\times10^7$ S/m were assumed). It is found that the simulated radiation efficiency at the design frequency of the stacked-patch antenna with the soft surface is about 88%, only 2% lower than that of the same stack-patch antenna without the soft surface. The measured gain was obtained by calibrating the stacked-patch antennas with a standard gain horn antenna. From Fig. 10, we can see that the simulated broadside gain around the design frequency of the stacked-patch antenna with the soft surface is more than 9.0 dBi, about 6.5 dB improvement as compared to the stacked-patch without the soft surface. This gain improvement is also near 2 dB higher than that obtained for the single patch on a thinner substrate as described in the previous section. This is due to the contribution from the thicker substrate with the help of a soft surface: the thicker substrate excites stronger surface waves while the soft surface blocks and transforms the excited surface waves into space waves. Due to the frequency shift, the maximum

gain measured for the stacked patch with the soft surface is observed around 17 GHz and its value is near 9 dBi, almost 7 dB higher than the gain at broadside for the stacked-patch antenna without the soft surface. Note for comparison that the gain improvement measured in [11] is only 3 dB in the broadside direction for a patch antenna (on a substrate with ε_r=10.2) surrounded by three UC-PBG (uniplanar compact photonic bandgap) periods (about $1.1\lambda_g$).

IV. Conclusion

The effectiveness of a modern soft surface concept on the radiation-pattern improvement of a patch antenna on a large-size substrate has been investigated. The new soft surface structure consists of a ring of short-circuited metal strips with a strip width of a quarter guided wavelength, much more compact than typical PBG/EBG structures. It has been demonstrated that the broadside gain of the patch antenna surrounded by the compact soft surface can be increased by about 5 dB while the backside level is reduced by almost 8 dB. The mechanism for the radiation-pattern improvement has been analyzed and it has been revealed that the optimal length of the soft surface ring is approximately one wavelength in free space plus the patch size. The compact soft surface structure can be easily implemented in 3D modules, such as those fabricated using LTCC technology. Experimental results show that it is feasible to make use of the via-metallization process on the LTCC technique for realization of a shorting wall required by the compact soft surface structure. A maximum gain of near 9 dBi can be achieved at broadside for a patch antenna on a thick and large-size LTCC substrate.

Acknowledgement

The authors wish to acknowledge the support of Georgia Electronics Design Center, the NSF CAREER Award under contract NSF #9964761, and the NSF Packaging Research Center, the NASA project under contract #NCC3-1015, and the NSF Award NSF ECS-0313951. The authors also would like to thank Dr. S. Pinel for his help in LTCC process.

References

[1] J.-Y. Park, S.-S. Jeon, Y. Wang. And T. Itoh, "Integrated antenna with direct conversion circuitry for broad-band millimeter-wave communications," *IEEE Trans. Microwave Theory Tech.,* vol. 51, no. 5, pp. 1482-1488, May 2003.

[2] J. Huang, "Finite ground plane effects on microstrip antenna radiation patterns," *IEEE Trans. Antennas Propagat*., vol. 31, pp. 649-653, Apr. 1983.

[3] 9. A. Bokhari, J. R. Mosig, and F. E. Gardiol, "Radiation pattern computation of microstrip antennas on finite size ground planes," *IEE Proc.-H*, vol. 139, no. 3, pp. 278-286, 1992.

[4] S. Maci, L.Borelli, and L. Rossi, "Diffraction at the edge of a truncated grounded dielectric slab," *IEEE Trans. Antennas Propagat*., vol. 44, pp. 863-872, June 1996.

[5] M. Stotz, G. Gottwald, and H. Haspeklo, "Planar millimeter wave antennas using SiN_x-membrances on GaAs," *IEEE Trans. Microwave Theory Tech.,* vol. 44, no. 9, pp. 1593-1596, Sept. 1996.

[6] J.-G. Yook and P. B. Katehi, "Micromachined microstrip patch antenna with controlled mutual coupling and surface waves," *IEEE Trans. Antennas Propagat*., vol. 49, pp. 1282-1289, Sept. 2001.

[7] D. Moongilan, "Grounding optimization techniques for controlling radiation and crosstalk in mixed signal PCBs," *Proceedings of IEEE Electromagnetic Compatibility Symposium*, vol. 1, pp. 495-500. Aug. 1998.

[8] M. O. Thieme and E. M. Biebl, "Calculation of the surface-wave excitation in multilayered structures," *IEEE Trans. Antennas Propagat*., vol. 46, pp. 686-693, May 1998.

[9] M. J. Vaughan, K. Y. Hur, and R. C. Compton, "Improvement of microstrip patch antenna radiation patterns," *IEEE Trans. Antennas Propagat*., vol. 42, no. 6, pp. 882-885, June 1994.

[10] R. Gonzalo, P. de. Maagt, and M. Sorolla, "Enhanced patch-antenna performance by suppressing surface waves using photonic-bandgap substrates," *IEEE Trans. Microwave Theory Tech.,* vol. 47, no. 11, pp. 2131-2138, Nov. 1999.

[11] R. Coccioli, F.-R. Yang, K.-P. Ma, and T. Itoh, "Aperture-coupled patch antenna on UC-PBG substrate," *IEEE Trans. Microwave Theory Tech.,* vol. 47, no. 11, pp. 2123-2130, Nov. 1999.

[12] D. Sievenpiper, L. Zhang, R. F. J. Broas, N. G. Alexopolous, and E. Yablonovitch, "High-impedance electromagnetic surfaces with forbidden frequency band," *IEEE Trans. Microwave Theory Tech.,* vol. 47, no. 11, pp. 2059-2074, Nov. 1999.

[13] H.-Y. D. Yang, J. Wang, "Surface waves of printed antennas on planar artificial periodic dielectric structures," *IEEE Trans. Antennas Propagat*., vol. 49, no. 3, pp. 444-450, Mar. 2001.

[14] Y.-J. Park, A. Herschlein, and W. Wiesbeck, "A photonic bandgap (PBG) structure for guiding and suppressing surface waves in millimeter-wave antennas," *IEEE Trans. Microwave Theory Tech.,* vol. 49, no. 10, pp. 1854-1859, Oct. 2001.

[15] M. Rahman and M. A. Stuchly, "Circularly polarized patch antenna with periodic structure," *IEE Proc-Microw. Antenna Progag*., vol. 149, no. 3, June 2002.

[16] R. B. Hwang and S. T. Peng, "Surface-wave suppression of resonance-type periodic structures," *IEEE Trans. Antennas Propagat*., vol. 51, no. 6, pp. 1221-1229, June 2003.

[17] J. S. Colburn and Y. Rahmat-Samii, "Patch antennas on externally perforated high dielectric constant substrates," *IEEE Trans. Antennas Propagat*., vol. 47, no. 12, pp. 1785-1794. Dec.1999.

[18] D. R. Jackson and J. T. Williams, and A. K. Bhattacharyya, "Microstrip patch designs that do not excite surface waves," *IEEE Trans. Antennas Propagat*., vol. 41, no. 8, pp. 1026-1037, 1993.

[19] J. Papapolymerou, R. F. Drayton, and L. P. B. Katehi, "Micromachined patch antennas," *IEEE Trans. Antennas Propagat*., vol. 46, no. 2, pp. 275-283, Feb. 1998.

[20] P.-S. Kildal, "Artificially soft and hard surfaces in electromagnetics,", *IEEE Trans. Antennas Propagat*., vol. 38, no.10, , pp. 1537-1544, 1990.

[21] Z. Ying and P.-S. Kildal, "Improvements of dipole, helix, spiral, microstrip patch and aperture antennas with ground planes by using corrugated soft surfaces," *IEE Proc.-Microw. Antennas Propag*., vol. 143, no. 3, pp. 244-248, 1996.

[22] R. L. Li, G. DeJean, M. Tentzeris, J. Laskar, and J. Papapolymerou, "LTCC multiplayer based CP patch antenna surrounded by a soft-and-hard surface for GPS applications," *Proceedings of IEEE Antenna and Propagation Society International Symposium*, vol. 2, pp. 651-654, June 2003.

[23] G. Ruvio, P.-S. Kildal, and S. Maci, "Modal propagation in ideal soft and hard waveguides," *Proceedings of IEEE Antenna and Propagation Society International Symposium*, vol. 4, pp. 438-441, June 2003.

[24] R. Garg, P. Bhartia, I. Bahl, and A. Ittipiboon, *Microstrip antenna design handbook*, Norwood, MA, Artech House, pp. 265-269, 2001.

[25] M. Tentzeris, R. L. Li, K. Lim, M. Maeng, E. Tsai, G. DeJean, and J. Laskar, "Design of Compact Stacked-Patch Antennas on LTCC Technology for Wireless Communication Applications," *Proceedings of IEEE Antenna and Propagation Society International Symposium*, vol. 2, pp. 500-503, June 2002.

List of Figure Captions

Fig. 1. Patch antenna surrounded by an ideal compact soft surface structure which consists of a ring of metal strip and a ring of shorting wall (I_s=the surface current on the top surface of the soft surface ring, Z_s=the impedance looking into the shorted metal strip).

Fig. 2. Directivity of the soft-surface-surrounded patch antenna as a function of the inner length (L_s) of the soft surface ring with W_s= 2.65, 1.88, and 1.36 mm for ε_r=2.9, 5.4, and 9.6, respectively.

Fig. 3. Directivity of the soft-surface-surrounded patch antenna as a function of frequency with optimized W_s= 2.65, 1.88, and 1.36 mm and optimized L_s= 24, 22, and 20 mm for ε_r=2.9, 5.4, and 9.6, respectively.

Fig. 4. Comparison of return loss between the patch antennas with and without the soft surface (ε_r=2.9, x_p=1.9 mm).

Fig. 5. Comparison of radiation-patterns in principal planes between the patch antennas with and without the soft surface (ε_r =9.6, f_0=15 GHz).
(a) E-plane (ϕ=0°)
(b) H-plane (ϕ=90°)

Fig. 6. Simulated electric field distributions on the top surface of the substrate for the patch antennas with and without the soft surface (ε_r =9.6).
(a) With soft surface
(b) Without soft surface

Fig. 7. Layout and prototype of a stacked-patch antenna surrounded by a compact soft surface structure implemented on LTCC technology.
(a) Layout
(b) Prototype

Fig. 8. Comparison of return loss between simulated and measured results for the stacked-patch antennas with and without the soft surface implemented on LTCC technology.
(a) With soft surface
(b) Without soft surface

Fig. 9. Comparison between simulated and measured radiation patterns for the stacked-patch antennas with and without the soft surface implemented on LTCC technology (f_0=17 GHz).
(a) E-plane (ϕ=0°)
(b) H-plane (ϕ=90°)

Fig. 10. Comparison of simulated and measured gains at broadside between the stacked-patch antennas with and without the soft surface implemented on LTCC technology.

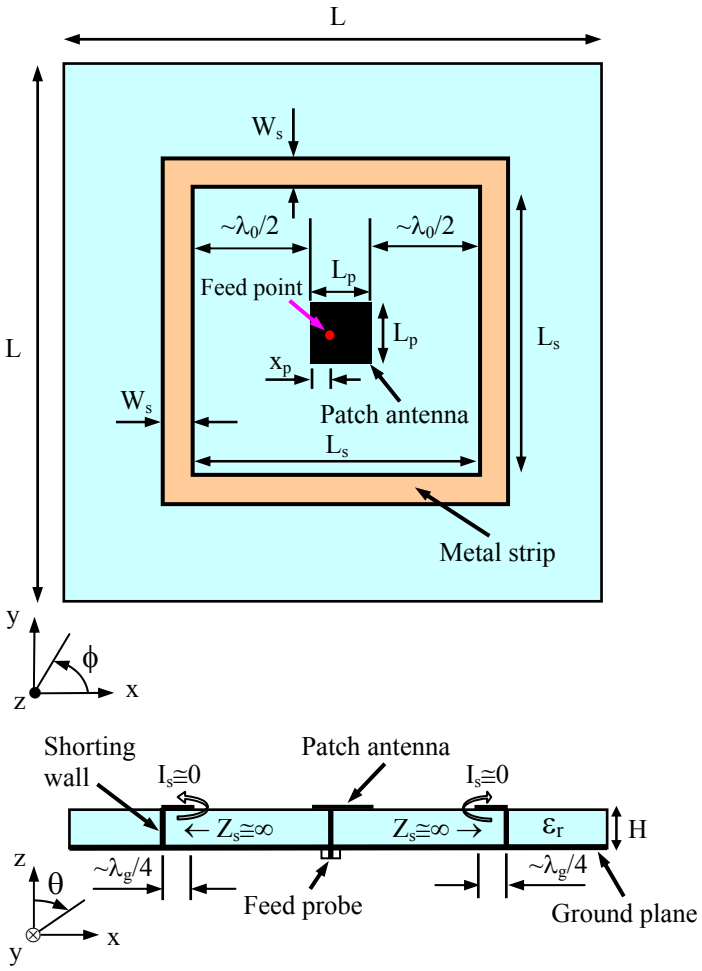

Fig. 1. Patch antenna surrounded by an ideal compact soft surface structure which consists of a ring of metal strip and a ring of shorting wall (I_s=the surface current on the top surface of the soft surface ring, Z_s=the impedance looking into the shorted metal strip).

.

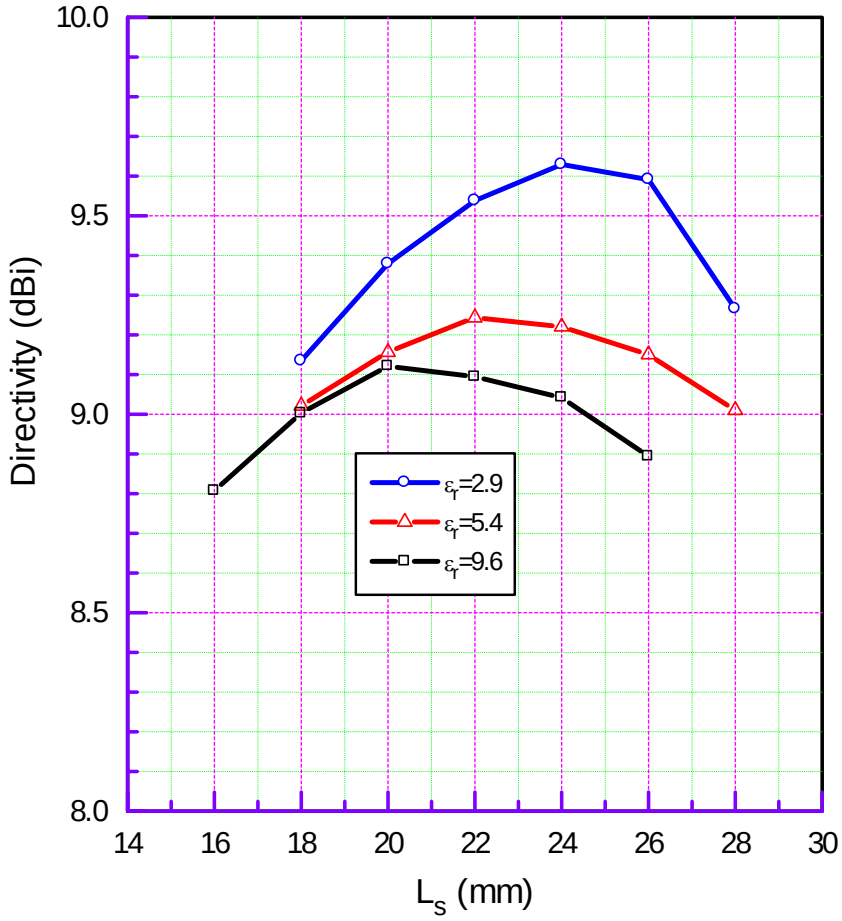

Fig. 2. Directivity of the soft-surface-surrounded patch antenna as a function of the inner length (L_s) of the soft surface ring with W_s= 2.65, 1.88, and 1.36 mm for ε_r=2.9, 5.4, and 9.6, respectively.

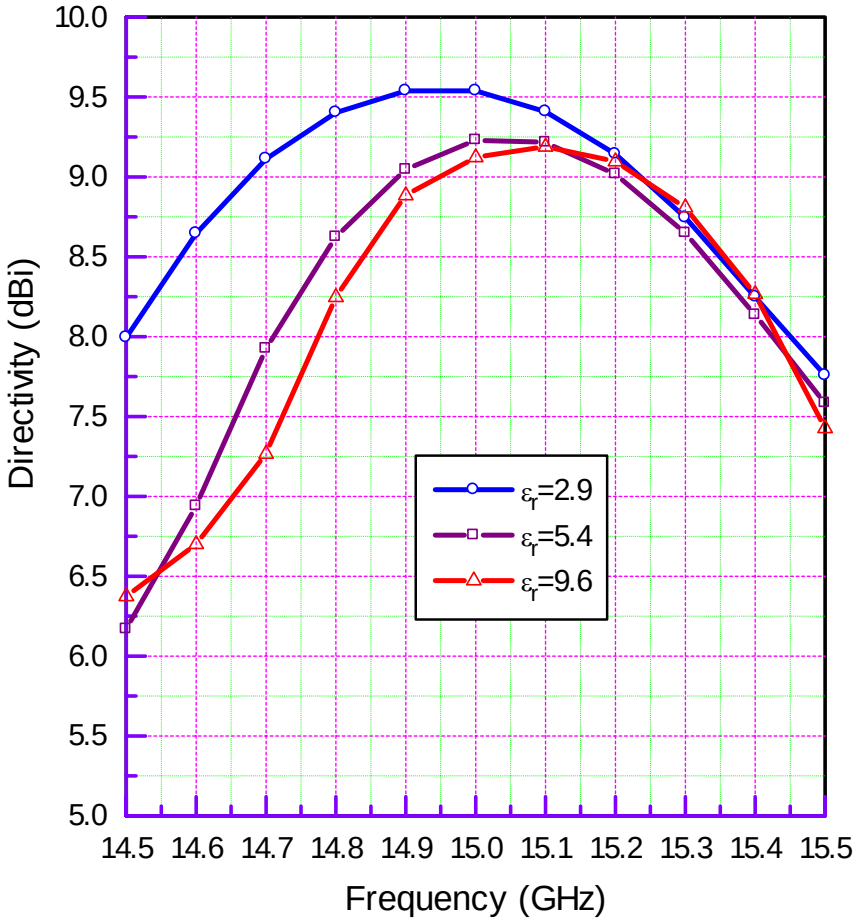

Fig. 3. Directivity of the soft-surface-surrounded patch antenna as a function of frequency with optimized W_s= 2.65, 1.88, and 1.36 mm and optimized L_s= 24, 22, and 20 mm for ε_r=2.9, 5.4, and 9.6, respectively.

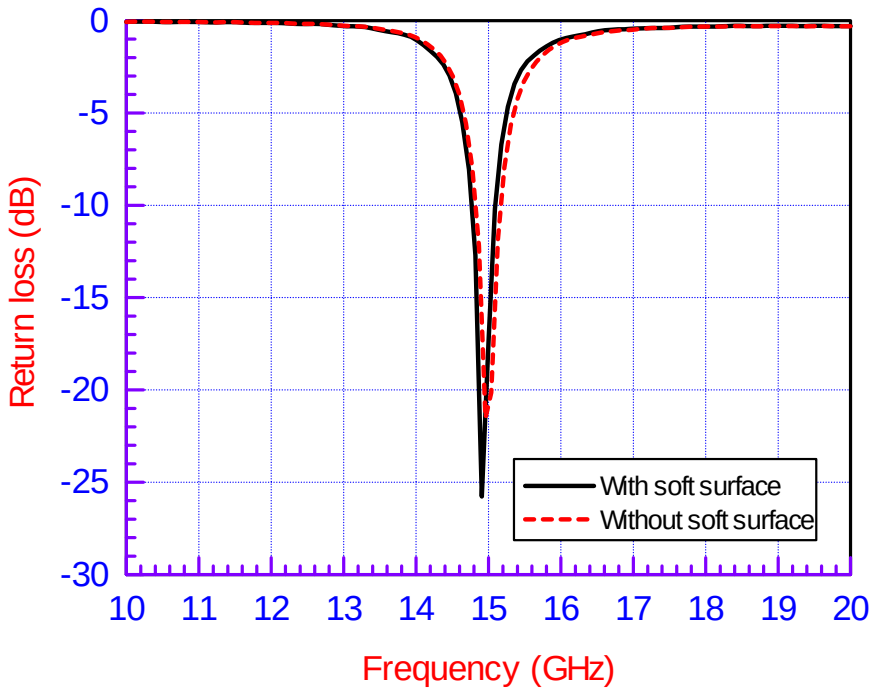

Fig. 4. Comparison of return loss between the patch antennas with and without the soft surface (ε_r=2.9, x_p=1.9 mm).

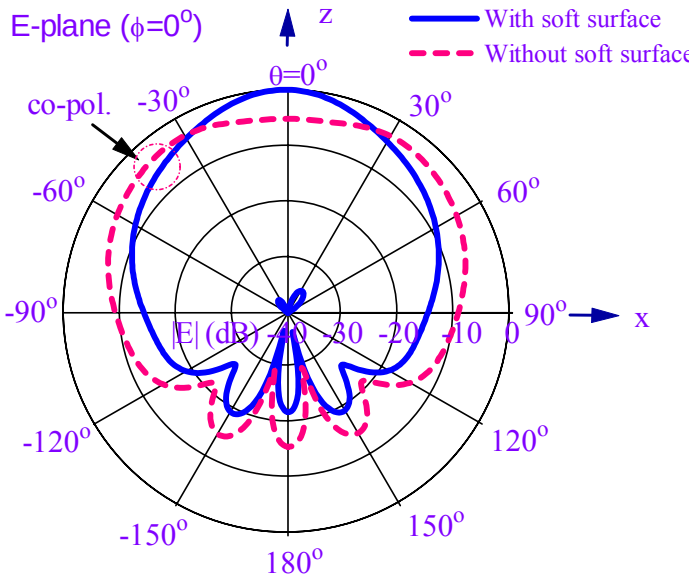

(a) E-plane (ϕ=0°)

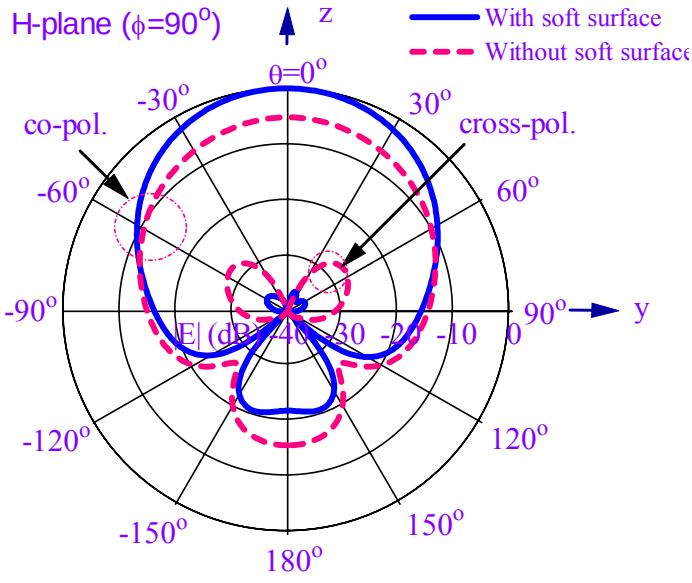

(b) H-plane (ϕ=90°)

Fig. 5. Comparison of radiation-patterns in principal planes between the patch antennas with and without the soft surface (ε_r =9.6, f_0=15 GHz).

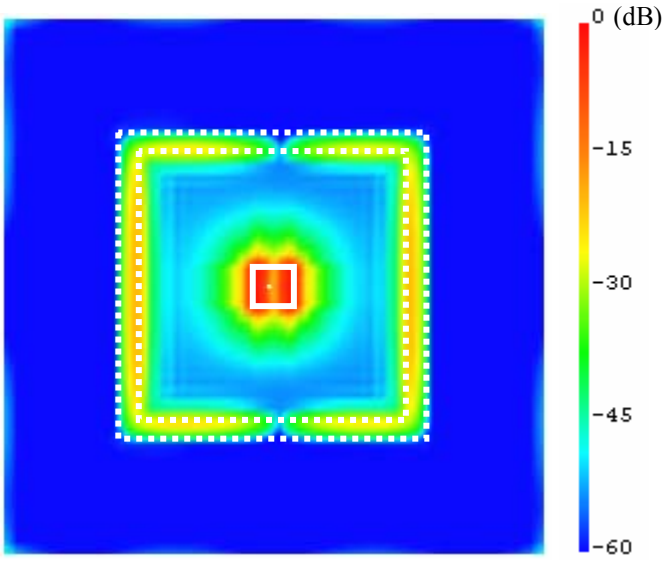

(a) With soft surface

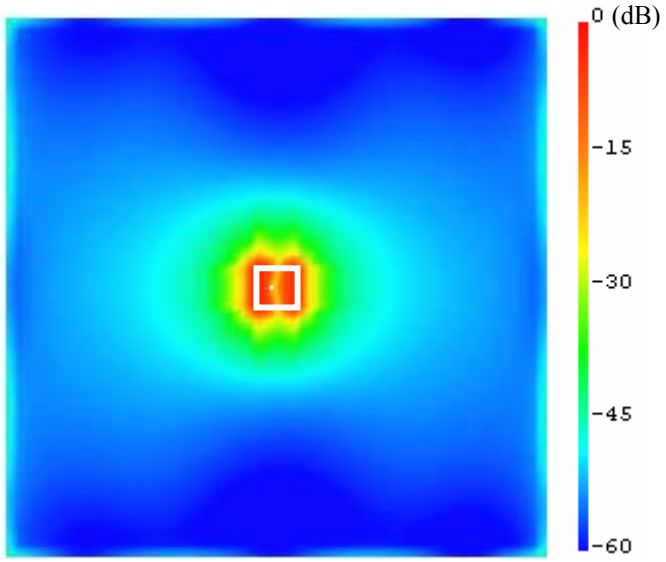

(b) Without soft surface

Fig. 6. Simulated electric field distributions on the top surface of the substrate for the patch antennas with and without the soft surface (ε_r =9.6).

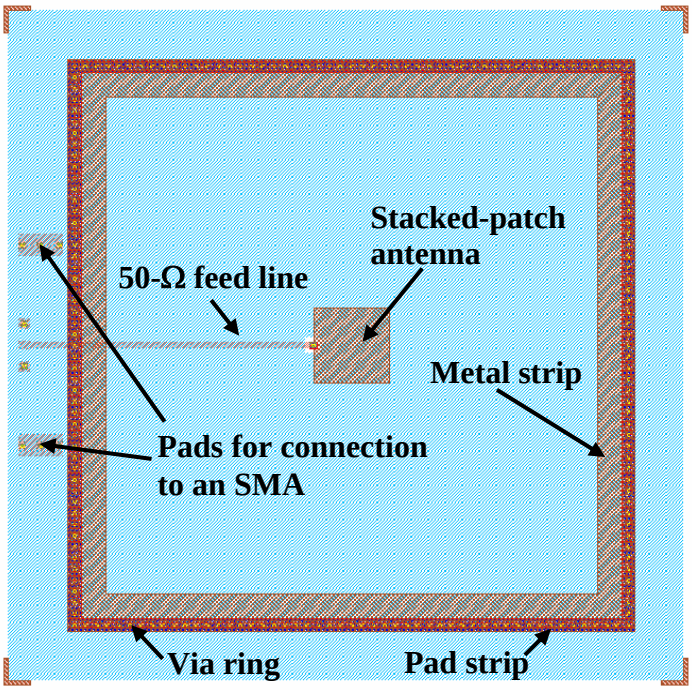

(a) layout

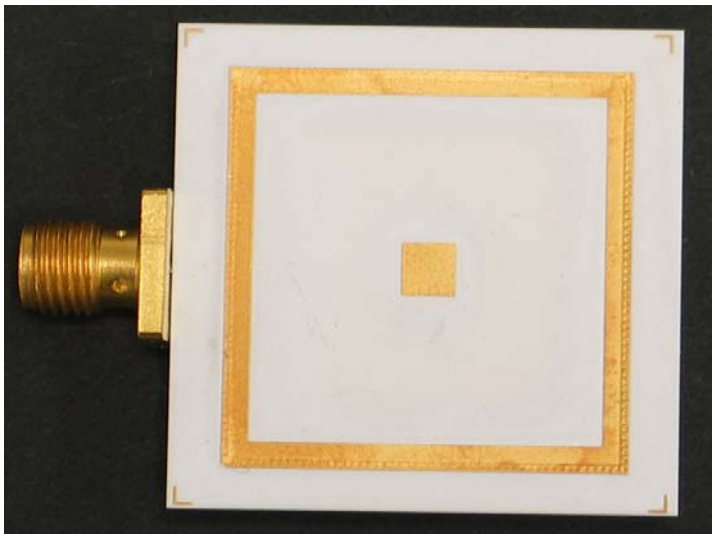

(b) Prototype

Fig. 7. Layout and prototype of a stacked-patch antenna surrounded by a compact soft surface structure implemented on LTCC technology.

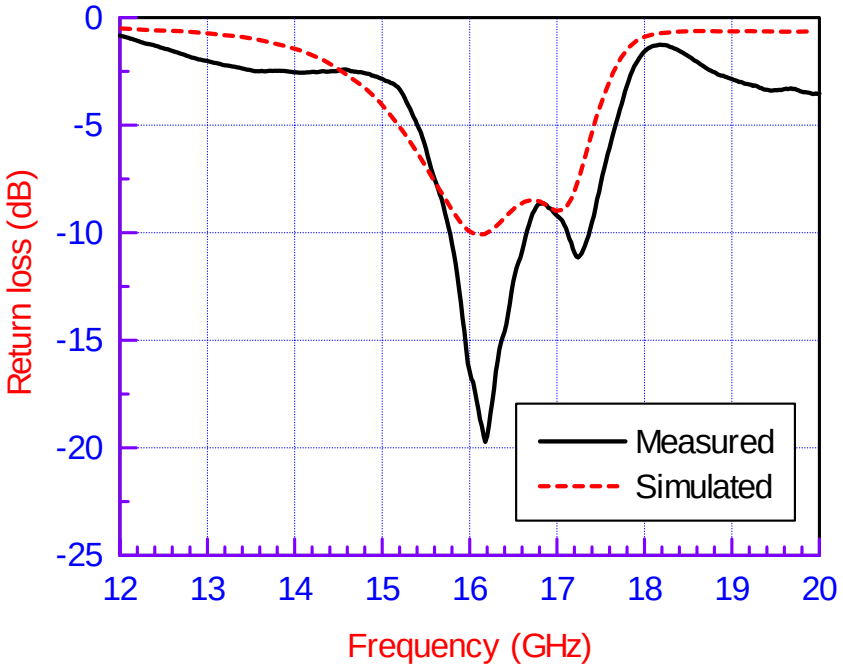

(a) With soft surface

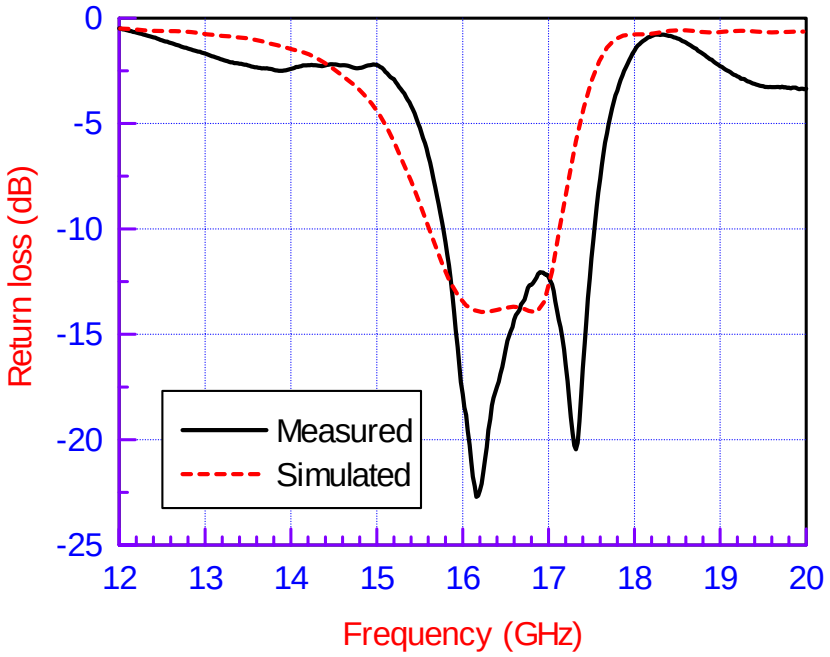

(b) Without soft surface

Fig. 8. Comparison of return loss between simulated and measured results for the stacked-patch antennas with and without the soft surface implemented on LTCC technology.

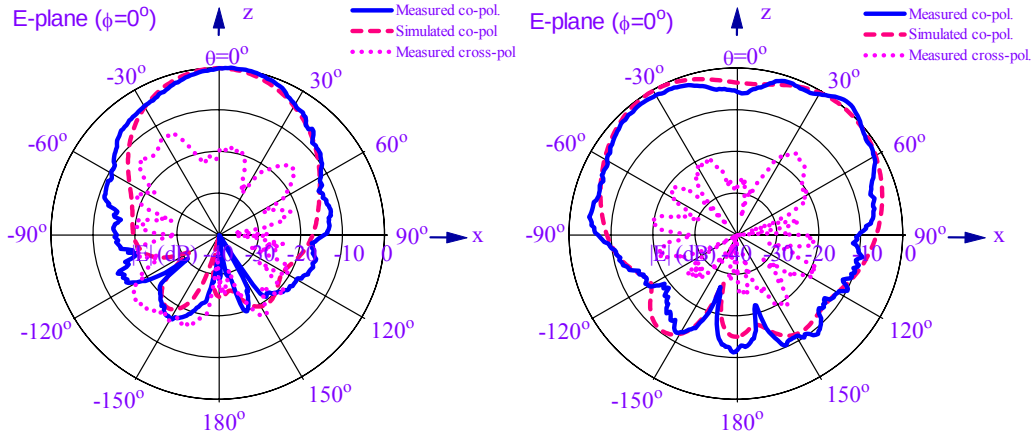

With soft surface Without soft surface

(a) E-plane (ϕ=0°)

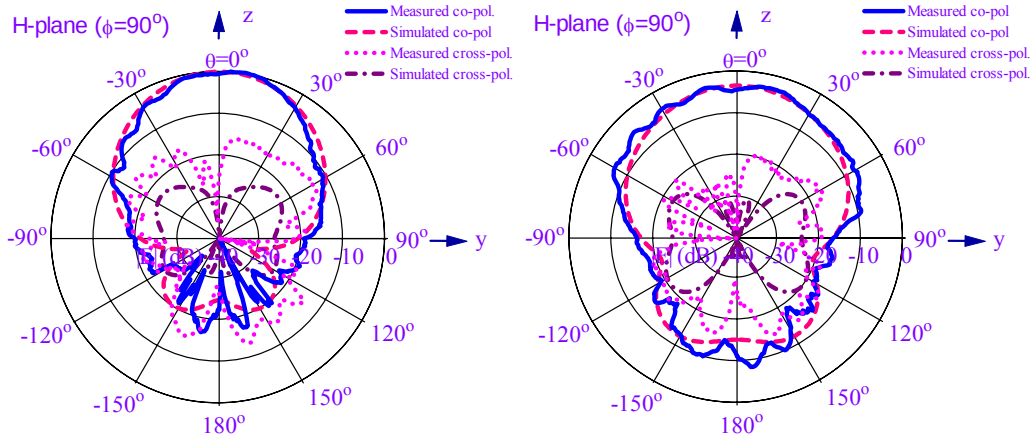

With soft surface Without soft surface

(b) H-plane (ϕ=90°)

Fig. 9. Comparison between simulated and measured radiation patterns for the stacked-patch antennas with and without the soft surface implemented on LTCC technology (f_0=17 GHz).

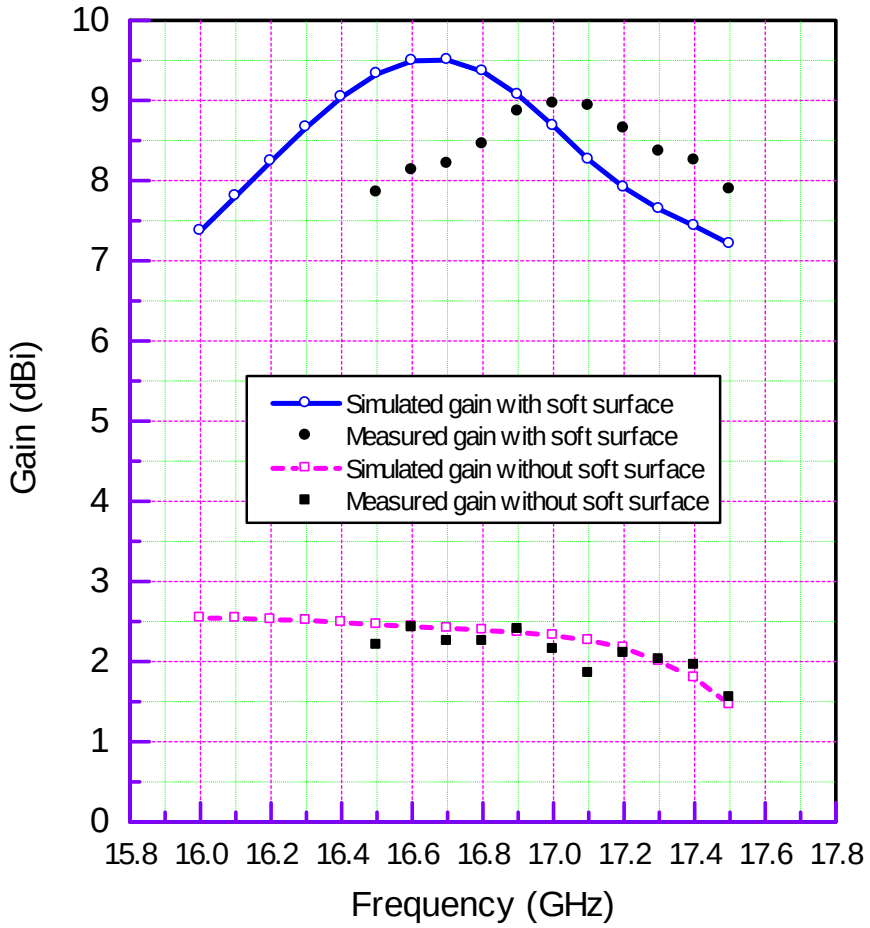

Fig. 10. Comparison of simulated and measured gains at broadside between the stacked-patch antennas with and without the soft surface implemented on LTCC technology.